Article Volume 15, Issue 6, 2025, 84

https://doi.org/10.33263/BRIAC156.084

From Synthesis to Bioactivity: A Ti(IV)-Coordinated Phosphorylated Schiff Base System with XRD-Validated Structure and Enhanced Efficacy Against Multidrug-Resistant Bacterial Pathogens

Dheya A. Hameed ¹, Nedhal A. A. Al-Selwi ¹, Fathi M. Al-Azab ¹, Yasmin M.S. Jamil ^{1,*}, Ahmed N Alhakimi ², Gamil M.S. Qasem ^{1,3}, Thamer Alorini ², Abuzar E. A. Albadri ²

- Chemistry Department, Faculty of Science, Sana'a University, Sana'a, Yemen
- ² Department of Chemistry, College of Sciences, Qassim University, Buraidah-51452, Saudi Arabia.
- ³ Chemistry Department, Faculty of Applied Sciences, Thamar University, Yemen
- * Correspondence author: y.jamil@su.edu.ye;

Received: 1.04.2025; Accepted: 5.08.2025; Published: 14.11.2025

Abstract: novel organophosphorus Schiff base ligand, diphenyl (2-((2phenylhydrazineylidene)methyl)phenyl) phosphate (OPSBL), was synthesized through the reaction of 2-(2-phenylhydrazineylidene)methyl phenol with diphenylchlorophosphate. Its Ti(IV) complex, [Ti(OPSBL)Cl₂]Cl₂·2H₂O, was prepared in a 1:2 molar ratio (metal: ligand) and characterized via IR, UV-Vis, ¹H/¹³C NMR, XRD, and elemental analysis. The complex exhibited electrolytic behavior, as confirmed by molar conductance measurements (134.18 Ω^{-1} cm² mol⁻¹). XRD analysis revealed reduced crystallinity (41%) and smaller particle size (~300 nm) compared to the ligand, attributed to structural disarray and disrupted intermolecular interactions upon metal coordination. Molecular docking studies against Staphylococcus aureus (4URM), Bacillus subtilis (2RHL), and Escherichia coli (4PRV) demonstrated strong binding affinities (-6.00 to -6.52 kcal/mol), particularly targeting resistance-associated enzymes. Antibacterial assays against multidrug-resistant pathogens showed superior inhibitory activity for the Ti(IV) complex vs. the free ligand (25 mm vs. 18 mm at 300 µg/mL against E. coli. These findings highlight the potential of Ti(IV)-Schiff base systems as a preliminary indication of multi-target potential against resistant bacterial infections, combining structural stability with bioactivity. Further studies on cytotoxicity and single-crystal validation are warranted.

Keywords: titanium (IV) complex; organophosphorus Schiff base; IR spectra; XRD; molecular docking; antibacterial activity.

© 2025 by the authors. This article is an open-access article distributed under the terms and conditions of the Creative Commons Attribution (CC BY) license (https://creativecommons.org/licenses/by/4.0/), which permits unrestricted use, distribution, and reproduction in any medium, provided the original work is properly cited. The authors retain copyright of their work, and no permission is required from the authors or the publisher to reuse or distribute this article, as long as proper attribution is given to the original source.

1. Introduction

Through their diverse applications, organophosphorus compounds and their complex Ti (VI) derivatives have impacted various scientific fields, including chemistry, medicine, materials science, and agriculture, particularly as insecticides. Several research papers have been published on their synthesis since 1990 [1-5]. In some organophosphorus compounds, as nerve or chemical warfare agents [6-8]. Due to their utility in industrial and biological applications, numerous Schiff bases with complexes have been thoroughly investigated and

assessed [9, 10]. Since Rosenberg discovered the platinum-based cisplatin in 1970, the function of transition metal complexes in medicinal chemistry has been well understood [11, 12]. Transition metal complexes have been investigated as antibacterial agents [13, 14], anticancer agents [15, 16], and catalysts for various catalytic activities [17–19] in recent years. Coordination complexes have demonstrated thermodynamic and kinetic properties that favor biological receptors due to their distinct coordination spheres, oxidation states, and redox potentials.

Titanocene dichloride, a non-platinum-based medicine that utilizes titanium, has been developed as an anticancer medication [20, 21]. Titanocene dichloride demonstrated anti-inflammatory, anti-arthritic, and antiviral qualities in addition to its anticancer capabilities [22]. Titanium should be integrated into living systems because it is present in various biomaterials, including food and the pigment in lightning [23]. The development of novel medications that exhibit improved action due to bacterial resistance to currently existing antibiotics is attracting increasing interest [24, 25]. Metals and ligands can be utilized to create or discover new medications, as they have diverse effects on the life cycle of pathogens [26, 27]. Furthermore, due to their enhanced coordination behavior, ligands containing atoms of nitrogen, oxygen, and phosphorus are known to exhibit notable biological activity [28, 29]. Because of their enhanced lipophilicity, inhibition of enzymes, and interaction with intracellular biomolecules, metal complexes are recognized as antimicrobial agents following chelation [30–32].

While Ti(IV)-Schiff base systems are known [5], their efficacy against MDR strains remains underexplored. Recent phosphoryl-containing analogs [3,34] exhibit enhanced bioavailability, but none combine a phenylhydrazine backbone with diphenyl phosphate groups—a design we hypothesize will improve target engagement. Notably, prior studies [33–36] used model bacteria; here, we test clinical MDR isolates.

This study presents a new Ti(IV)-organophosphorus Schiff base complex featuring bidentate (N, O) coordination, which is optimized for both thermal stability (>300°C) and antibacterial efficacy. It is positioned as a preliminary indication of multi-target potential against resistant infections, as molecular docking demonstrates a better binding affinity (-6.52 kcal/mol) against *S. aureus* compared to analogues [35]. This study fills the gaps in the current literature regarding efficacy and mechanism by combining synthesis, spectrum analysis, and computational insights [36] to develop a titanium-based antibacterial design.

2. Materials and Methods

2.1. Material.

Metal salt, phenyl hydrazine, and ortho-hydroxybenzaldehyde were acquired from BHD. Diphenylchlorophosphate and tri-ethylamine were acquired from Riedel-de Haen, while solvents of spectroscopic purity were employed.

2.2. Synthesis of OPSBL.

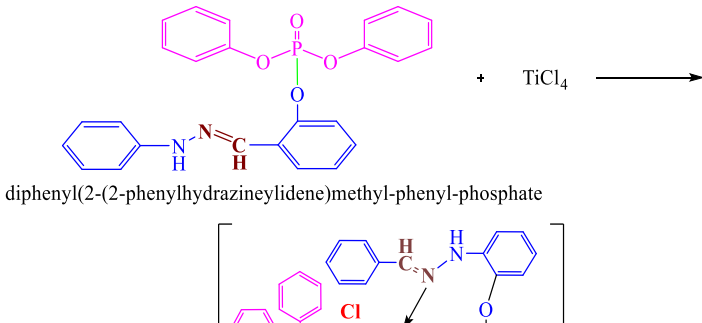
An absolute acetonitrile (50 ml) solution of Schiff base (4.24 g, 0.02 mol) was combined with a solution of diphenyl chlorophosphate (5.37 ml, 0.02 mol) in acetonitrile (50 ml) to create the OPSBL, which had a molar ratio of 1:1 and triethylamine (2.78 ml, 0.02 mol) present (Scheme 1). After the reaction mixture was completely added, it was refluxed for approximately three to five hours. The product was recovered by filtering out the solid (triethylamine hydrochloride), and then the solvent was evaporated in a water bath.

 $diphenyl (2\hbox{-}(2\hbox{-phenylhydrazineylidene}) methyl\hbox{-phenyl-phosphate}$

Scheme 1. Synthesis of OPSBL.

2.3. Synthesis of titanium (VI) complex.

20 ml of ethanol was utilized to dissolve 4 mmol (1.46 g) of OPSBL individually. It was added to a solution of ethanol (20 ml) with 2 mmol of TiCl₄ (0.19 g). The mixture was refluxed at 60° to 70°C for almost three hours while being constantly stirred. After precipitation, the OPSBL solid metal complex was left to cool to ambient temperature. After filtering it out, petroleum ether was used for washing. Hot ethanol was used to recrystallize the dried complex. Scheme 2 illustrates the synthesis of the Titanium(IV) complex of OPSBL.



 $\begin{array}{c|c} & H & H \\ \hline C_{N} & O \\ \hline O & P = O \\ \hline O & N \\ \hline C & H \\ \end{array}$ $Cl_{2}.2H_{2}O$

Scheme 2. Synthesis of Ti (VI) complex.

2.4. Methods and instrumentation.

A Jenway model 4510 conductivity meter was used to measure the molar conductance of a 10⁻³M solution of the metal complex in DMSO solvent. The measurement was performed at room temperature using freshly prepared solutions. The melting points of the ligand and its complex were measured in degrees Celsius using a Stuart Scientific electrothermal melting point apparatus in glass capillary tubes. At the University of Sana'a, the electronic spectra of the substances in the 200–800 nm range were measured using a UV-VIS spectrophotometer (Analytic Jena, Germany). The compounds' 200–4000 cm⁻¹ infrared spectra were measured using an instrument (FT/IR-140, Jasco, Japan). The concentration of metal was measured using a Perkin-Elmer 2380 flame atomic absorption spectrophotometer. NMR spectra were obtained at 25°C at 850 MHz and 213 MHz using a Bruker spectrometer. A Rigaku XRD diffractometer (Ultima IV, USA) was utilized to collect the XRD patterns of the compounds. The anode material, Cu Ka (k = 1.54180 Å), functioned at 30 mA of current and 40 kV of voltage. Science

Faculty, Al Qasim University. The C, H, and N analyses of the chemical were performed in Vario EL Fab. CHN No. 11042023 at the Central Laboratory, Faculty of Science, Cairo University, Egypt. Using silver nitrate, chloride was measured gravimetrically [37]. The weight loss approach was used to gravimetrically measure the quantity of uncoordinated water molecules [37].

2.5. XRD data on particle size and crystallinity.

The percentage of crystallinity, XC (%), was computed using the integrated peak areas of the main peaks [34, 38]. The complex's crystallinity is determined as a ratio to the ligand's crystallinity:

$$X_C(\%) = \frac{A complex}{A ligand} \times 100(1)$$

where the regions under the principal peaks of the complex and ligand samples are indicated by A $_{complex}$ and A $_{ligand}$, respectively.

X-ray diffraction was also used to measure the average particle size (D), which was calculated using the Scherrer equation [39, 40].

$$D = \frac{K\lambda}{\beta \cos \theta} \tag{2}$$

Assuming that λ is the X-ray wavelength of Cu-K α radiation (1.5405 Å), β is the full width at half maximum (FWHM), θ is the Bragg diffraction angle in degrees, and K is the Scherrer constant, which equals 0.94.

- 2.6. Bioassay studies.
- 2.6.1. Molecular docking methodology.
- 2.6.1.1. Compound preparation.

It was discovered that the [Ti(OPSBL)Cl₂].Cl₂,2H₂O complex exhibited a strong cytotoxic action against microbial strains.

Initially, the MMFF94x force field with reaction-field electrostatics (Din = 1, Dout = 80) was used to construct and reduce the complex's three-dimensional structure. A flat-bottom tether (10.0 kcal/mol, 0.25 Å) was used to tether every atom. All adjustments were performed using MOE software [41]. Second, the database was created by converting the complex's structure into format.mdb, which was then used as the input for the MOE-docking simulation.

2.6.1.2. Protein preparation.

Three distinct X-ray crystal structures were obtained from the Protein Data Bank (http://www.rcsb.org/pdb/) and used as the antibacterial targets. The proteins from *S. aureus* [42], *S. pyogenes* [43], and *E. coli* [44] have PDB IDs of 4URM, 5XYR, and 4PRV, respectively. We retained each target's A chain while removing the water molecules, ions, and cofactors from the structures to facilitate the simulation. After adjusting the intended structures for missing atoms, the hydrogen atoms were added [45].

2.6.1.3. Molecular docking protocol.

Computational molecular docking was used to identify how medicines interact with the target's active site residues. The docking experiments in our study were carried out using the

Molecular Operating Environment (MOE) software [41]. We followed the same simulation protocols as previous research [35, 46, 47]. For docking, the following parameters were used: London dG was the Rescoring 1 function, while Triangle Matcher was the placement method.

The selected target proteins—*Staphylococcus aureus* (PDB ID: 4URM), *Streptococcus pyogenes* (PDB ID: 5XYR), and *Escherichia coli* (PDB ID: 4PRV)—were prioritized based on their direct involvement in bacterial antibiotic resistance mechanisms. For instance, 4URM (Gyrase B) is a key enzyme in DNA replication targeted by fluoroquinolones, and mutations in this protein are linked to quinolone resistance [42]. Similarly, 5XYR (a penicillin-binding protein) mediates β-lactam resistance in *S. pyogenes* [43], while 4PRV (a multidrug efflux pump component) facilitates antibiotic expulsion in *E. coli* [44]. These targets were retrieved from the Protein Data Bank (PDB) and validated against recent literature highlighting their roles in resistance pathways [48].

2.6.2. Antibacterial assay.

Three microorganisms, *Staphylococcus aureus*, *Pseudomonas aeruginosa*, and *E. coli*, were used to test the antibacterial properties of the synthesized Organophosphorus Schiff base and its complex. The antibacterial activity was assessed using the Agar well diffusion method [33, 49]. Stock solutions containing 1000 µg/ml were created using DMSO as the solvent. These were then used to prepare concentrations of 100, 200, and 300 µg/ml, respectively. The bacteria were placed on the surface of the nutritional agar. On the surface of the nutritional agar, the bacteria were introduced. The wells and ditches made on the agar plates were inoculated with the chemicals in varying quantities. For 24 hours, the plates were incubated at 37 °C. Gentamicin 120 µg/ml was used as a reference, and the results were recorded by measuring the diameter of the inhibitory zone (mm). To ensure the reliability of the findings, all experiments were performed in triplicate, and statistical significance was assessed using Student's *t*-test (p < 0.05). The calculated standard deviation (SD) for inhibition zones ranged between ± 1.2 and 1.8 mm, confirming minimal variability across replicates.

3. Results and Discussion

Following the preparation of a novel bioactive ligand (OPSB) and its Ti (IV) complex, the methods from the literature were used. The proposed structure of the compounds was in good agreement with the complex's molecular weight and the micro-elemental assays for C, H, N, and M. The resulting compounds were stable and had color. The complex's molar conductance value of 134.18 Ω^{-1} cm² mol-1 in DMSO (1 × 10 ³ M) 1:2 demonstrates its electrolytic behavior [33].

Table 1 presents the analytical data. Schemes 1 and 2 provide an overview of the complicated and suggested structure of OPSBL and its complexity.

Compound	Color	M.P Λ m (Ω^{-1} F. Wt.			Element analysis calculated% (Found)				
Compound	(Yield)	(C °)	cm ² mol ⁻¹)	(g/mole)	C	H	N	P	Ti
OPSBL	Dark green 78.18	245	-	444.43	67.56 (67.50)	4.76 (4.70)	6.30 (6.44)	6.97 (6.88)	-
[Ti (OPSBL)Cl ₂] Cl ₂ .2H ₂ O	Light green 63.22	346	134.18	1114.62	59.60 (59.54)	4.20 (4.18)	5.56 (5.67)	6.15 (6.17)	4.75 (4.79)

Table 1. Analysis of the OPSBL and its complex's physical characteristics and elements.

3.1. Spectroscopic studies.

3.1.1. ¹H–NMR spectroscopic studies.

With CDCl₃ as a solvent, the ^{1}H NMR spectrum of the ligand in DMSO-d₆ (Figure 1) was determined. The aromatic protons were detected at ($\delta = 6.761$ -7.561) ppm (multiple) in the ^{1}H NMR spectrum. The signal of aromatic aldehydes at (8.172) ppm (s, 1H) produced the azomethine proton (N=CH) [50]. The proton of the N-H imine group is responsible for the singlet signals at ($\delta = 10.674$) ppm [51].

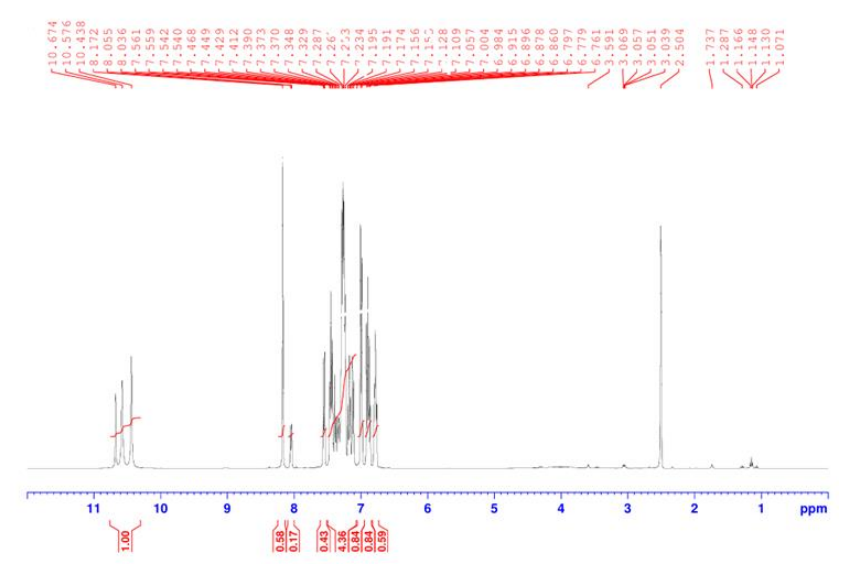


Figure 1. 1H-NMR spectrum of OPSBL.

3.1.2. ¹³C–NMR spectroscopic studies.

A singlet signal at 167.41 ppm in the ¹³C NMR spectrum (Figure 2) could be attributed to the azomethine carbon (C=N) [52]. The methylene group's carbon was detected at 59.22 ppm. The number of peaks in OPSBL that are ascribed to aromatic carbon ranges from 116.93 to 132.83 ppm [53].

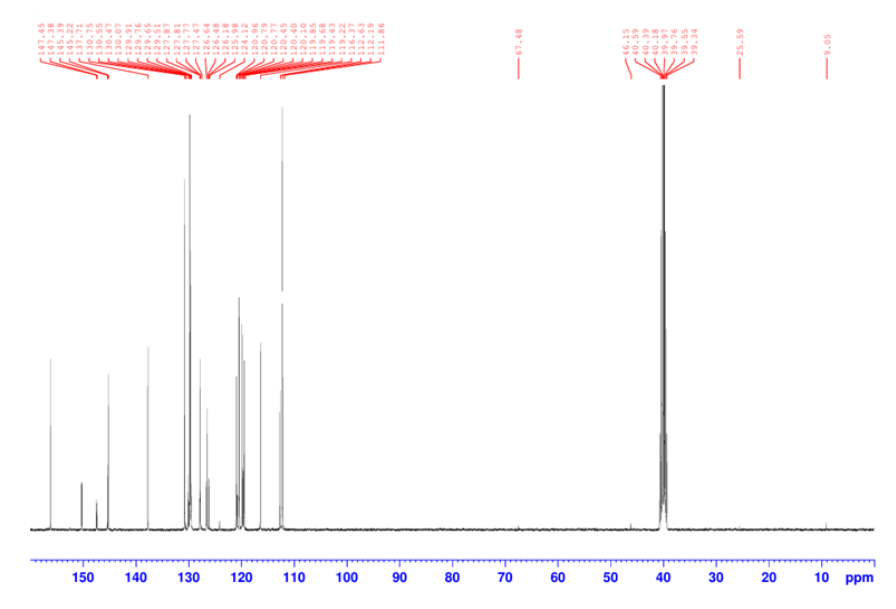


Figure 2. ¹³C- NMR spectrum of OPSBL.

3.1.3. Electronic spectroscopic studies.

The 200–800 nm region of the ligand's OPSB and its metal complex's electronic spectra data in DMSO solution. The absorbance bands at 312 and 359 nm in the ligand UV-Vis spectrum (Figure 3) may be associated with OPSBL (dark green) and its complex (light green), [Ti(OPSBL)Cl₂]Cl₂.2H₂O, which is shown in Figure 3. The n- π * transition is associated with bands at about 310–355 nm. Additionally, bands in the 300–360 nm range are designated as LMCT [54, 55]. Bands observed between 270 and 310 nm are classified as π - π * type transitions [56]. The n- π * transition of the nonbonding electrons on the nitrogen of the azomethine group in the Organophosphorus Schiff base causes the electronic absorption bands to move to lower energy [51]. According to these findings, the metal ion and the imine nitrogen atom seem to be coordinated [56]. Chelation caused these bands to shift to a shorter wavelength, confirming the development of the complex. Because of LMCT, it was challenging to distinguish spectral bands that arise in complexes from n- π * transition bands. Most significantly, the d^0 -state of the Ti(IV) complex is confirmed by the absence of any peak above 500 nm, which indicates a d-d transition.

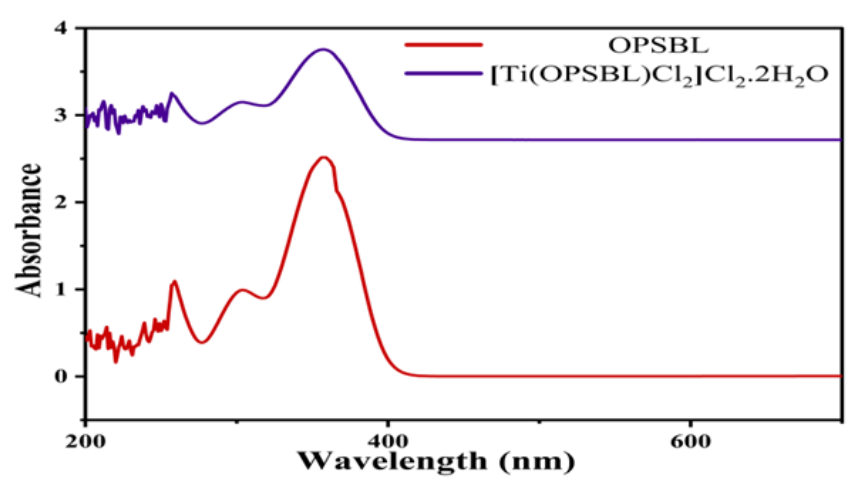


Figure 3. UV-Vis spectrum of OPSBL and its complex.

3.1.4. FTIR spectroscopic studies.

In the FTIR spectrum of the free OPSBL ligand (Figure 4), the C=N stretching vibration was observed at 1645 cm⁻¹. Upon complexation with Ti(IV), this band shifted to 1602 cm⁻¹, indicating a red shift of ~43 cm⁻¹. This shift is attributed to the coordination of the azomethine nitrogen atom (N) to the Ti⁴⁺ ion, which withdraws electron density from the C=N bond, weakening its strength and lowering the stretching frequency. Such a red shift is a hallmark of metal-ligand coordination and aligns with studies on analogous Schiff base-Ti(IV) complexes [57-59]. The P=O stretching band in the ligand appeared at 1188 cm⁻¹ but shifted to 1155 cm⁻¹ in the Ti(IV) complex, showing a red shift of ~33 cm⁻¹. This suggests coordination of the phosphoryl oxygen atom (O) to the Ti⁴⁺ ion, redistributing electron density within the P=O bond and reducing its stiffness. The simultaneous coordination of both N (from C=N) and O (from P=O) confirms the bidentate binding mode of OPSBL, forming a stable octahedral geometry around the Ti(IV) center (Figure 4 and Table 2). The existence of υ(P=O) and υ(P-O-C) is indicated by the emergence of bands at 1188 cm⁻¹ and 1100 cm⁻¹, respectively [33]. At 3081 cm⁻¹ is the aromatic C-H stretching band. The aromatic C=C stretching band, on the other hand, is situated at 1512 cm⁻¹. The new 400-600 cm⁻¹ vibrations that are not present in the free are believed to be caused by v(M-N) and v(M-Cl) [52] (Figure 4 and Table 2).

Table 2. The main IR bands of the OPSBL and its complex.

Compounds	υ (C=N)	υ (P=O)	υ (P-O-C)	υ(C=C)	υ (-NH)	υ (M-N)
OPSBL	1645	1188	1100	1512	3373	-
[Ti (OPSBL)Cl ₂]Cl ₂ .2H ₂ O	1602	1155	1074	1502	3362	496

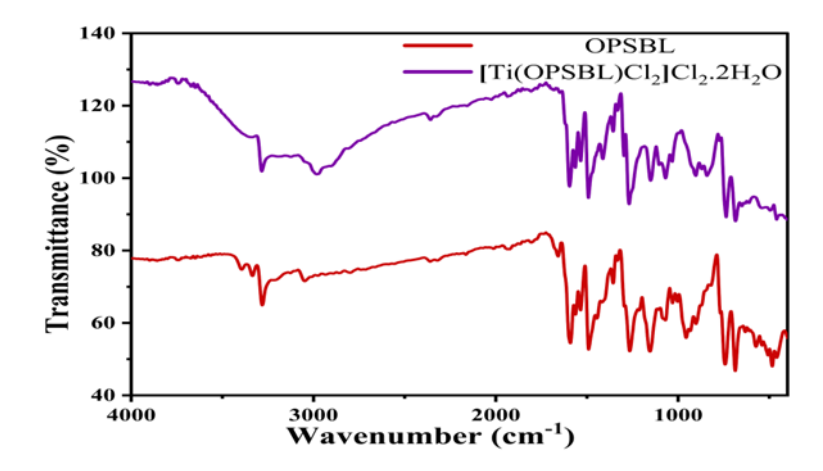


Figure 4. Infrared frequencies of the OPSBL and its complex.

3.1.5. X-ray diffraction.

Figure 5 displays the OPSBL and its complex's XRD patterns. The reduction in crystallinity based on the complexation is responsible for a decrease in the XRD peak intensities of the OPSBL complex [60, 61]. This corresponds well with the complex's measured decrease in relative crystallinity (Relative crystallinity is determined by finding the integrated area of the complex's principal peaks to the OPSBL, summarized in Table 3 [38].

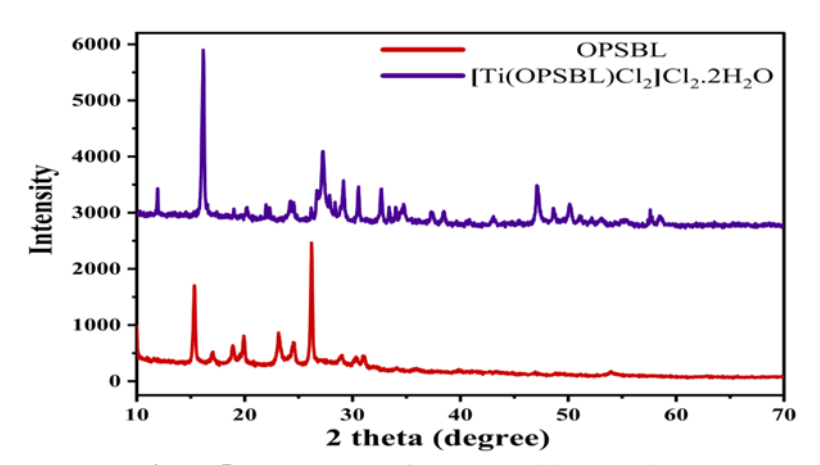


Figure 5. XRD pattern of OPSBL and its complex.

The XRD patterns revealed a significant decrease in crystallinity for the Ti(IV) complex (41% relative crystallinity) compared to the free ligand (100%). This phenomenon is explained by the following factors.

3.1.5.1. Structural disarray from metal coordination.

The incorporation of the Ti⁴⁺ ion into the ligand framework disrupts the long-range crystalline order of OPSBL. The presence of chloride counterions (Cl⁻) and water molecules (H₂O) in the complex ([Ti(OPSBL)Cl₂]Cl₂·2H₂O) introduces steric and electronic distortions, further reducing crystallinity [38].

3.1.5.2. Disruption of intermolecular interactions.

In the free ligand, hydrogen bonding and π - π stacking between aromatic rings stabilize the crystalline lattice. Upon complexation, these interactions are weakened due to the steric bulk of the Ti(IV) center and the rigid coordination bonds, leading to a less ordered structure [62].

3.1.5.3. Particle size reduction.

Using the Scherrer equation, the average particle size (D) decreased from ~725 nm (ligand) to ~300 nm (complex) (Table 3). This reduction results from the fragmentation of crystalline domains during the coordination process, leading to smaller, less crystalline particles. Similar trends have been reported for metal-organic complexes with disrupted lattice symmetry [63].

Table 3. Principal intensity values of the OPSBL and its complex as determined by XRD spectrum.

Compound	2θ	В	D (nm)	Mean D	XC (%)
	19.000	0.070	1186.410		
	26.159	0.600	138.414		
	28.621	0.070	1166.430		
OPSBL	32.625	0.177	469.201	725.194	-
	48.608	0.170	1167.544		
	52.119	0.260	704.412		
	55.015	0.710	243.952		
	19.919	0.241	344.600		
[Ti (OPSBL)Cl ₂]Cl ₂ .2H ₂ O	28,984	0.184	451.351	299.920	41
	35.672	0.800	103.810		

3.2. Molecular docking simulation.

To begin validating the docking method, we re-docked each native ligand into its target and calculated the root-mean-square deviation (RMSD) and binding free energy (S score) (Table 4). This allows us to compare the affinity of compounds and targets, as well as determine the strength of their binds [36].

 Table 4. Properties of targets, energy score, and RMSD values.

_	Cells	Target ID	Amino acid number	Resolution (Å)	S score (kcal/mol)	RMSD (Å)
_	S.aureus	4URM	231	2.94	-6.7737	1.5335
	S.pyoggenis	5XYR	1647	2.80	-4.0832	1.9293
	E.coli	4PRV	398	2.00	-8.2668	1.9923

The [Ti(OPSBL)Cl₂]Cl₂·2H₂O complex was then docked into the active site residues for the microbial strains' targets. Finally, for the complex, eight top conformations were obtained, and the optimal pose was chosen based on its energy score. Table 5 describes the docking findings computation, including energy scores, kinds of interactions, and distances between the complex and the three targets.

The interaction created between the complex and the binding site of target proteins was also shown using the Discovery Studio Visualizer v17.2.2.0 software (DSV).

According to the literature [64-66], hydrogen bond distances between 2.5 and 3.1 Å are considered strong interactions, whereas those between 3.1 and 3.55Å are considered weak interactions.

residues of enzymes are targets of inicrobial strains.									
Target	S-score (kcal/mol)	Atom of a compound	Involved receptor atoms	Involved receptor residues	Categories	Type of interaction bond	Distance (Å)		
S.aureus PDB ID: 4URM	(4621	/	NH1	ARG84	Electrostatic	π-Cation	3.50		
		/	NH2	ARG84	Electrostatic	π- Cation	4.19		
	-6.4621	/	OE1	GLU58	Electrostatic	π- Anion	3.67		
		/	/	PRO87	Hydrphobic	π-Alkyl	4.67		
S.pyoggenis PDB ID: 5XYR		Cl	HE2	LYS1006	H-bond	Carbon H-bond	2.86		
		P	NZ	LYS1006	Electrostatic	Attractive Charge	5.56		
	-6.0029	/	NZ	LYS1006	Electrostatic	π-Cation	3.44		
		/	NZ	LYS1006	Electrostatic	π-Cation	4.86		
		/	OE1	GLU1567	Electrostatic	π- Anion	4.73		
		/	/	HIS1498	Hydrphobic	π- π -T-shaped	5.05		
		/	/	HIS1498	Hydrphobic	π- π -T-shaped	5.20		
		/	/	VAL1527	Hydrphobic	π-Alkyl	5.33		
E.coli PDB ID: 4PRV		О	HG	SER108	H-bond	Conventional H- bond	2.76		
		/	NH1	ARG136	Electrostatic	π-Cation	3.42		
	-6.5240	/	OD2	ASP105	Electrostatic	π- Anion	3.40		
		/	/	PRO84	Hydrphobic	π-Alkyl	4.71		
		/	/	ALA90	Hydrphobic	π-Alkyl	5.00		
		/	/	PRO79	Hydrphobic	π-Alkyl	4.11		

Table 5. Docking score and interactions between [Ti(OPSBL)Cl₂] Cl₂·2H₂O complex and the active site residues of enzymes are targets of microbial strains.

It is apparent from Table 5 that the development of hydrogen bonds and electrostatic interactions according to molecular docking computational results in the complex demonstrated good inhibition of the (PDB ID: 5XYR) *S. pyoggenis* and (PDB ID: 4PRV) *E. coli* target proteins, while there was weak inhibition with the (PDB ID: 4URM) *S. aureus* target protein, with energy score: -6.0029, -6.5240 and -6.4621 Kcal/mol respectively (see Figures 6–11).

We note that in the case of *S. aureus* target (PDB: 4URM), a complex was formed with three electrostatic interactions (Table 5+Figures 6 and 7).

[Ti(OPSBL)Cl₂].Cl₂·2H₂O complex forms one strong hydrogen bond with the active site residue of *S. pyogenes* target (PDB: 5XYR): Cl/LYS1006-HE2/bond distance= 2.86 Å, and four electrostatic interactions (Table 5, Figures 8 and 9).

Finally, this complex and the major residue of the $E.\ coli$ target (PDB: 4PRV) formed one hydrogen bond: O/SER108-HG/bond distance = 2.76 Å, and two electrostatic interactions (Table 5, Figures 10 and 11).

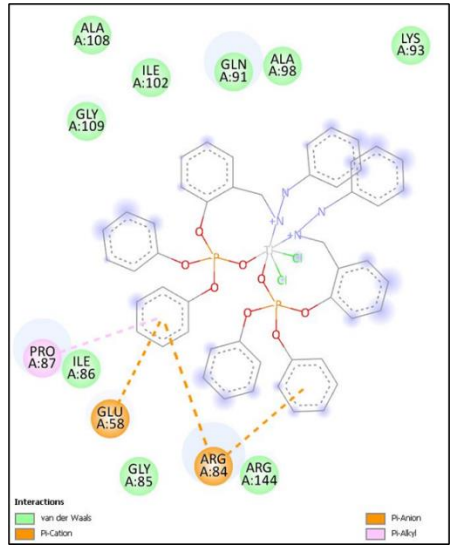


Figure 6. 2D plot of interaction of [Ti (OPSBL)Cl₂]Cl₂.2H₂O complex and the active site residues of (4URM) enzyme of *S. aureus*.

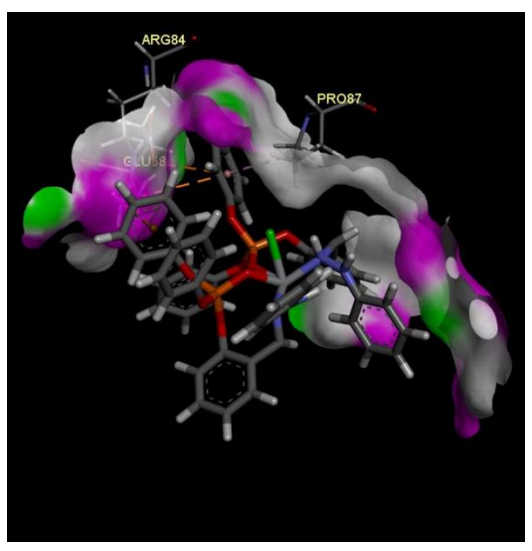


Figure 7. 3D plot of the interaction of [Ti (OPSBL)Cl₂] Cl₂.2H₂O complex and the active site residues of (4URM) enzyme of *S. aureus*.

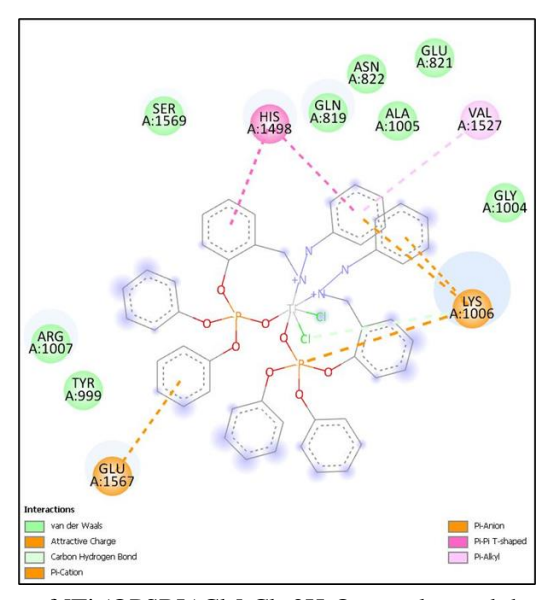


Figure 8. 2D plot of interaction of [Ti (OPSBL)Cl₂] Cl₂.2H₂O complex and the active site residues of (5XYR) enzyme of *S. pyogenes*.

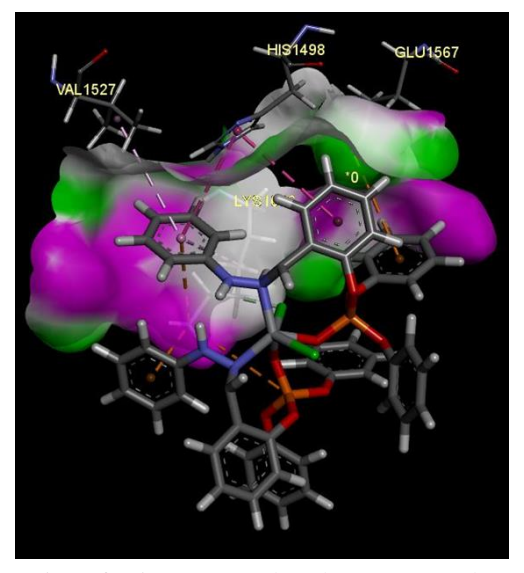


Figure 9. 3D plot of the interaction of [Ti (OPSBL)Cl₂] Cl₂.2H₂O complex and the active site residues of (5XYR) enzyme of *S. pyogenes*.

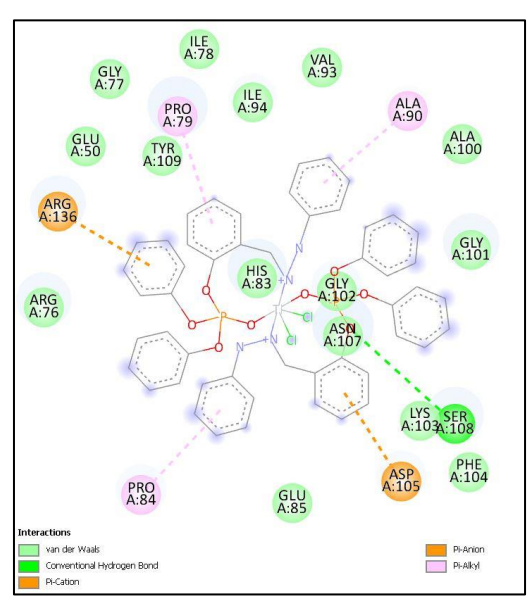


Figure 10. 2D plot of the interaction of [Ti (OPSBL)Cl₂] Cl₂.2H₂O complex and the active site residues of (4PRV) enzyme of *E. coli*.

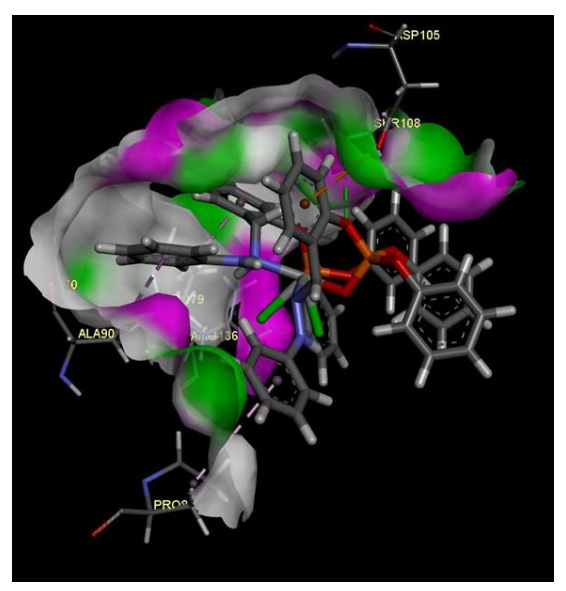


Figure 11. 3D plot of the interaction of [Ti (OPSBL)Cl₂] Cl₂.2H₂O complex and the active site residues of (4PRV) enzyme of *E. coli*.

3.3. Antibacterial studies.

Using the bacteria *S. aureus*, *S. sapogenins*, and *E. coli*, the synthesized Organophosphorus Schiff base and its complex were investigated for their antibacterial properties. The antibacterial activity was assessed using the agar well diffusion method [33, 49]. Table 6 and Figure 12 present the results:

Table 6. OPSBL and its complex's impact on bacterial growth (Zone of inhibition in millimeters).

Compounds	Conc. [µg/ml]	Staphylococcus aureus	S. Sapogenin	E. coli
	100	10	10	11
OPSBL	200	18	15	18
	300	25	18	15
	100	10	11	14
[Ti(OPSBL)Cl ₂]Cl ₂ .2H ₂ O	200	22	15	22
	300	23	22	25
Gentamicin	300	32	30	30

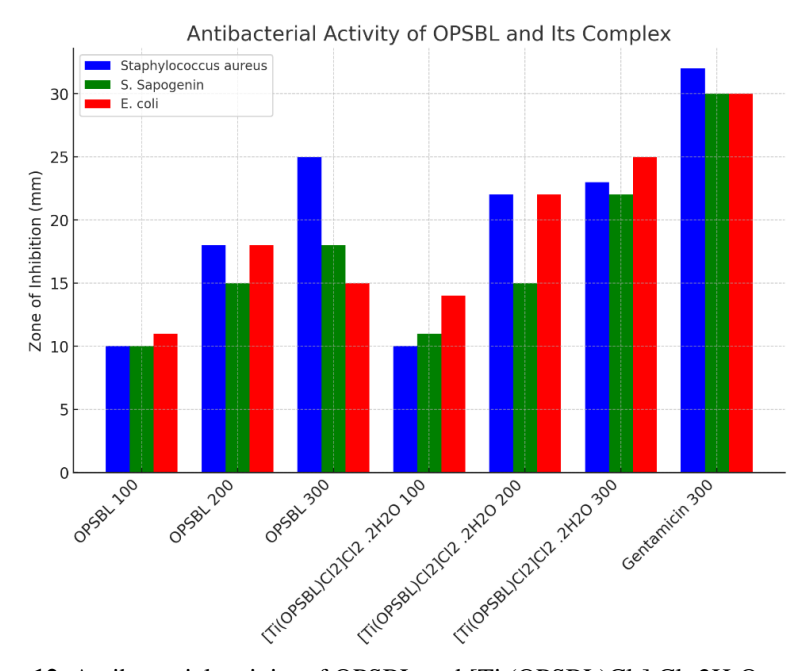


Figure 12. Antibacterial activity of OPSBL and [Ti (OPSBL)Cl₂] Cl₂.2H₂O complex.

4. Conclusions

A novel organophosphorus Schiff base ligand (2-((2-phenylhydrazineylidene) methyl)phenyl) phosphate (OPSBL) and its Ti(IV) complex, [Ti(OPSBL)Cl₂]Cl₂ .2H₂O, were synthesized and characterized. The ligand, featuring unique N, O-bidentate coordination sites, formed an octahedral Ti(IV) complex, as confirmed by spectral and XRD analyses, which revealed reduced crystallinity (41%) and a smaller particle size (~300 nm). Molecular docking revealed a strong binding affinity (-6.00 to -6.52 kcal/mol) against the targets of *S. aureus*, *E. coli*, and *S. pyogenes*. Antibacterial assays demonstrated that the new ligand-complex system outperformed the free ligand, with inhibition zones up to 25 mm at 300 μg/mL. This study introduces a structurally distinct ligand and highlights Ti(IV)-Schiff base complexes as promising antimicrobial agents. Further work should address cytotoxicity and structural validation via single-crystal XRD.

Author Contributions

Conceptualization, D.A.H., F.M.A., Y.M.S.J.; methodology, F.M.A., Y.M.S.J.; software, G.M.S.Q., T.A., A.E.A.A.; validation, D.A.H., N.A.A.S., A.N.A., G.M.S.Q.; formal analysis, N.A.A.S., Y.M.S.J., A.N.A.; investigation, Y.M.S.J., F.M.A., A.N.A., G.M.S.Q., T.A., A.E.A.A.; data curation, G.M.S.Q., T.A.; writing—original draft preparation, Y.M.S.J., N.A.A.S., G.M.S.Q., T.A.; writing—review and editing, Y.M.S.J., N.A.A.S.; visualization, D.A.H., F.M.A., Y.M.S.J.; supervision, D.A.H., F.M.A., Y.M.S.J.; project administration, F.M.A., Y.M.S.J. All authors have read and agreed to the published version of the manuscript.

Institutional Review Board Statement

Not applicable.

Informed Consent Statement

Not applicable.

Data Availability Statement

Data supporting the findings of this study are available upon reasonable request from the corresponding author.

Funding

This research received no external funding.

Acknowledgments

This research has no acknowledgment.

Conflicts of Interest

The authors declare that they have no conflict of interest.

References

- 1. Tiankun, Z.; Peng, W.; Xupeng, Z.; Nan, L.; Wenzhuo, Z.; Yong, Z.; Pengpeng, Y.; Shanjia, L.; Mingjun, Y.; Zhongduo, Y.; Thomas, H. Anti-tumoral Titanium^(IV) Complexes Stabilized with Phenolato Ligands and Structure-Activity Relationship. *Curr. Top. Med. Chem.* **2023**, 23, 1835-1849, https://doi.org/10.2174/1568026623666230505104626.
- 2. Eremeev, R.O.; Beznos, O.V.; Efremov, A.M.; Chesnokova, N.B.; Lozinskaya, N.A. The rational design of novel 5-amino-2-oxindole derivatives with antiglaucomic activity. *Bioorg. Med. Chem. Lett.* **2023**, *90*, 129334, https://doi.org/10.1016/j.bmcl.2023.129334.
- 3. Kaboudin, B.; Behroozi, M.; Sadighi, S.; Asgharzadeh, F. Recent Advances in the Electrochemical Synthesis of Organophosphorus Compounds. *Beilstein J. Org. Chem.* **2025**, 21, 770–797. https://doi.org/10.3762/bjoc.21.61.
- 4. Noor, A. Synthesis and Structures of Ti^{III} and Ti^{IV} Complexes Supported by a Bulky Guanidinate Ligand. *Crystals* **2021**, *11*, 886, https://doi.org/10.3390/cryst11080886.
- 5. Ryken, S.A.; Schafer, L.L. N,O-Chelating Four-Membered Metallacyclic Titanium(IV) Complexes for Atom-Economic Catalytic Reactions. *Acc. Chem. Res.* **2015**, *48*, 2576-2586, https://doi.org/10.1021/acs.accounts.5b00224.
- 6. Corbridge, D.E.C. Phosphorus: Chemistry, Biochemistry and Technology, 6th Edition; CRC Press: Boca Raton, **2013**; https://doi.org/10.1201/b12961.
- 7. Delfino, R.T.; Ribeiro, T.S.; Figueroa-Villar, J.D. Organophosphorus compounds as chemical warfare agents: a review. *J. Braz. Chem. Soc.* **2009**, 20, 407–428, https://doi.org/10.1590/S0103-50532009000300003.
- 8. Murphy, P. Organophosphorus Reagents. (Oxford Univ. Press, Oxford, 2004).
- 9. Mezgebe, K.; Mulugeta, E. Synthesis and pharmacological activities of Schiff bases with some transition metal complexes: a review. *Med. Chem. Res.* **2024**, *33*, 439–463, https://doi.org/10.1007/s00044-024-03192-5.
- 10. Chaudhary, N.K.; Guragain, B.; Chaudhary, S.K.; Mishra, P. Schiff base metal complex as a potential therapeutic drug in medical science: A critical review. *BIBECHANA* **2021**, *18*, 214–230, https://doi.org/10.3126/bibechana.v18i1.29841.
- 11. Gürsoy, A.; Karalı, N. Synthesis and primary cytotoxicity evaluation of 3-[[(3-phenyl-4(3H)-quinazolinone-2-yl)mercaptoacetyl]hydrazono]-1H-2-indolinones. *Eur. J. Med. Chem.* **2003**, *38*, 633–643, https://doi.org/10.1016/S0223-5234(03)00085-0.
- 12. Mohammad Nasir, U.; Didarul Alam, C.; Md. Moniruzzman, R.; Md. Ershad, H. Metal Complexes of Schiff Bases Derived from 2-Thiophenecarboxaldehyde and Mono/Diamine as the Antibacterial Agents. *Mod. Chem.* **2014**, 2, 6-14, https://doi.org/10.11648/j.mc.20140202.11.
- 13. Camellia, F.K.; Ashrafuzzaman, M.; Islam, M.N.; Banu, L.A.; Kudrat-E-Zahan, M. Isoniazid Derived Schiff Base Metal Complexes: Synthesis, Characterization, Thermal Stability, Antibacterial and Antioxidant Activity Study. *Asian J. Chem. Sci.* **2022**, *11*, 23–36, https://doi.org/10.9734/ajocs/2022/v11i419131.

- 14. da Silva, C.M.; da Silva, D.L.; Modolo, L.V.; Alves, R.B.; de Resende, M.A.; Martins, C.V.B.; de Fátima, Â. Schiff bases: A short review of their antimicrobial activities. *J. Adv. Res.* **2011**, 2, 1-8, https://doi.org/10.1016/j.jare.2010.05.004.
- 15. Thakor, P.M.; Patel, R.J.; Verma, D.N.; Patel, J.D. Natural acid-catalyzed synthesis of 6,6'-(((3,3'-dimethoxy-[1,1'-biphenyl]-4,4'-diyl)bis(azanylylidene))bis(methanylylidene))bis(2,4-dichlorophenol), its conventionally synthesized metal complexes and their potential as biological agents. *Rasayan J. Chem.* **2023**, *16*, 61–68, https://doi.org/10.31788/RJC.2023.1618108.
- Klein, A.V.; Hambley, T.W. Platinum-Based Anticancer Agents. In Ligand Design in Medicinal Inorganic Chemistry; Storr, T., Eds.; John Wiley & Sons, Ltd: 2014; pp. 9-45, https://doi.org/10.1002/9781118697191.ch2.
- 17. Palma, V.; Ruocco, C.; Cortese, M.; Renda, S.; Meloni, E.; Festa, G.; Martino, M. Platinum-Based Catalysts in the Water Gas Shift Reaction: Recent Advances. *Metals* **2020**, *10*, 866, https://doi.org/10.3390/met10070866.
- 18. Osowole, A.A.; Oni, O.A.; Kenneth, O.; Titilayo, H.A. Synthesis, Spectral, Magnetic and In-Vitro Anticancer Properties of Some Metal (II) Complexes of 3-[2,4-dihydro-1H-inden-4-ylimino] methyl] napthalene-2-ol. *Int. Res. J. Pure Appl. Chem.* **2012**, 2, 211–220, https://doi.org/10.9734/IRJPAC/2014/1370.
- 19. Tu, J.-L.; Huang, B. Titanium in photocatalytic organic transformations: current applications and future developments. *Org. Biomol. Chem.* **2024**, 22, 6650-6664, https://doi.org/10.1039/D4OB01152J.
- 20. Kostova, I. Anticancer Metallocenes and Metal Complexes of Transition Elements from Groups 4 to 7. *Molecules* **2024**, *29*, 824, https://doi.org/10.3390/molecules29040824.
- 21. Chakraborti, A.K.; Bhagat, S.; Rudrawar, S. Magnesium perchlorate as an efficient catalyst for the synthesis of imines and phenylhydrazones. *Tetrahedron Lett.* **2004**, *45*, 7641–7644, https://doi.org/10.1016/j.tetlet.2004.08.097.
- 22. Dalpozzo, R.; Nardi, M.; Oliverio, M.; Paonessa, R.; Procopio, A. ChemInform Abstract: Erbium(III) Triflate Is a Highly Efficient Catalyst for the Synthesis of β-Alkoxy Alcohols, 1,2-Diols and β-Hydroxy Sulfides by Ring Opening of Epoxides. *ChemInform* **2010**, *41*, https://doi.org/10.1002/chin.201010036.
- 23. Naeimi, H.; Salimi, F.; Rabiei, K. Mild and convenient one pot synthesis of Schiff bases in the presence of P₂O₅/Al₂O₃ as new catalyst under solvent-free conditions. *J. Mol. Catal. A Chem.* **2006**, 260, 100–104, https://doi.org/10.1016/j.molcata.2006.06.055.
- 24. Barluenga, J.; Aznar, F.; Valdes, C. N-Trialkylsilylimines as Coupling Partners for Pd-Catalyzed C—N Bond-Forming Reactions: One-Step Synthesis of Imines and Azadienes from Aryl and Alkenyl Bromides. *ChemInform* **2004**, *35*, https://doi.org/10.1002/chin.200416085.
- 25. Barluenga, J.; Jiménez-Aquino, A.; Fernández, M.A.; Aznar, F.; Valdés, C. Multicomponent and one-pot synthesis of trisubstituted pyridines through a Pd-catalyzed cross-coupling/cross-coupling/cycloaddition sequence. *Tetrahedron* **2008**, *64*, 778–786, https://doi.org/10.1016/j.tet.2007.10.112.
- 26. Jiang, L.; Jin, L.; Tian, H.; Yuan, X.; Yu, X.; Xu, Q. Direct and mild palladium-catalyzed aerobic oxidative synthesis of imines from alcohols and amines under ambient conditions. *Chem. Commun.* **2011**, *47*, 10833–10835, https://doi.org/10.1039/C1CC14242A.
- 27. Huang, B.; Tian, H.; Lin, S.; Xie, M.; Yu, X.; Xu, Q. Cu(I)/TEMPO-catalyzed aerobic oxidative synthesis of imines directly from primary and secondary amines under ambient and neat conditions. *Tetrahedron Lett.* **2013**, *54*, 2861–2864, https://doi.org/10.1016/j.tetlet.2013.03.098.
- 28. Shiraishi, Y.; Ikeda, M.; Tsukamoto, D.; Tanaka, S.; Hirai, T. One-pot synthesis of imines from alcohols and amines with TiO₂ loading Pt nanoparticles under UV irradiation. *Chem. Commun.* **2011**, *47*, 4811–4813, https://doi.org/10.1039/C0CC05615D.
- 29. Largeron, M.; Fleury, M.-B. Bioinspired Oxidation Catalysts. *Science* **2013**, *339*, 43–44, https://doi.org/10.1126/science.1232220.
- 30. Lan, Y.-S.; Liao, B.-S.; Liu, Y.-H.; Peng, S.-M.; Liu, S.-T. Preparation of Imines by Oxidative Coupling of Benzyl Alcohols with Amines Catalysed by Dicopper Complexes. *Eur. J. Org. Chem.* **2013**, 2013, 5160–5164, https://doi.org/10.1002/ejoc.201300507.
- 31. Largeron, M. Protocols for the Catalytic Oxidation of Primary Amines to Imines. *Eur. J. Org. Chem.* **2013**, 2013, 5225-5235.
- 32. Bera, A.; Vennapusa, S.R. Triplet state generation followed by the excited-state intramolecular proton transfer in 3-sulfanylchromen-4-one. *J. Photochem. Photobiol. A Chem.* **2023**, *441*, 114700, https://doi.org/10.1016/j.jphotochem.2023.114700.

- 33. Al-Azab, F.M.; Jamil, Y.M.S.; Al-Selwi, N.A.A.; Alhakimi, A.N.; Hameed, D.A.; Qasem, G.M.S.; Albadri, A.E.A. Titanium Complex with New Schiff Base 4-(N, N-dimethylaminobenzylidene)-1-phenylsemicarbazide: Synthesis, Thermal, XRD, and Antibacterial properties. *Sana'a Univ. J. Appl. Res. Technol.* **2024**, *2*, 391-402, https://doi.org/10.59628/jast.v2i4.1145.
- 34. Jamil, Y.M.; Al-Azab, F.M.; Al-Selwi, N.A. Novel organophosphorus Schiff base ligands: Synthesis, characterization, ligational aspects, XRD and biological activity studies. *Eclética Quím.* **2023**, *48*, 36–53, https://doi.org/10.26850/1678-4618eqj.v48.3.2023.p36-53.
- 35. Kibou, Z.; Aissaoui, N.; Daoud, I.; Seijas, J.A.; Vázquez-Tato, M.P.; Klouche Khelil, N.; Choukchou-Braham, N. Efficient Synthesis of 2-Aminopyridine Derivatives: Antibacterial Activity Assessment and Molecular Docking Studies. *Molecules* **2022**, *27*, 3439, https://doi.org/10.3390/molecules27113439.
- 36. Jamil, Y.M.S.; Al-Azab, F.M.; Al-Selwi, N.A.; Alorini, T.; Al-Hakimi, A.N. Preparation, physicochemical characterization, molecular docking, and biological activity of a novel Schiff-base and organophosphorus Schiff base with some transition metal(II) ions. *Main Group Chem.* **2023**, 22, 337-362, https://doi.org/10.3233/MGC-220101.
- 37. Harvey, D. Modern Analytical Chemistry, 3rd Edition; McGraw-Hill: USA, 2022.
- 38. Shah, B.; Kakumanu, V.K.; Bansal, A.K. Analytical techniques for quantification of amorphous/crystalline phases in pharmaceutical solids. *J. Pharm. Sci.* **2006**, *95*, 1641–1665, https://doi.org/10.1002/jps.20644.
- 39. Nasiri, S.; Rabiei, M.; Palevicius, A.; Janusas, G.; Vilkauskas, A.; Nutalapati, V.; Monshi, A. Modified Scherrer equation to calculate crystal size by XRD with high accuracy, examples Fe₂O₃, TiO₂, and V₂O₅. *Nano Trends* **2023**, *3*, 100015, https://doi.org/10.1016/j.nwnano.2023.100015.
- 40. Jamil, Y.M.S.; Al-Azab, F.M.; Al-Selwi, N.A.A.; Al-Ryami, A.M.; Mlahia, M.R. Spectroscopic and biological studies of mixed ligand complexes of transition metal (II) ions with chloroquine and ketoprofen. *Sana'a Univ. J. Appl. Sci. Technol.* **2024**, 2, 53–64, https://doi.org/10.59628/jast.v2i1.801.
- 41. Al-Harazie, A.G.; Gomaa, E.A.; Zaky, R.R.; Abd El-Hady, M.N. Spectroscopic Characterization, Cyclic Voltammetry, Biological Investigations, MOE, and Gaussian Calculations of VO(II), Cu(II), and Cd(II) Heteroleptic Complexes. *ACS Omega* **2023**, *8*, 13605–13625, https://doi.org/10.1021/acsomega.2c07592.
- 42. Lu, J.; Patel, S.; Sharma, N.; Soisson, S.M.; Kishii, R.; Takei, M.; Fukuda, Y.; Lumb, K.J.; Singh, S.B. Structures of Kibdelomycin Bound to *Staphylococcus aureus* GyrB and ParE Showed a Novel U-Shaped Binding Mode. *ACS Chem. Biol.* **2014**, *9*, 2023-2031, https://doi.org/10.1021/cb5001197.
- 43. Happonen, L.; Collin, M. Immunomodulating Enzymes from *Streptococcus pyogenes*—In Pathogenesis, as Biotechnological Tools, and as Biological Drugs. *Microorganisms* **2024**, *12*, 200, https://doi.org/10.3390/microorganisms12010200.
- 44. Stanger, F.V.; Dehio, C.; Schirmer, T. Structure of the N-Terminal Gyrase B Fragment in Complex with ADP·P_i Reveals Rigid-Body Motion Induced by ATP Hydrolysis. *PLoS ONE* **2014**, *9*, e107289, https://doi.org/10.1371/journal.pone.0107289.
- 45. Daoud, I.; Melkemi, N.; Salah, T.; Ghalem, S. Combined QSAR, molecular docking and molecular dynamics study on new Acetylcholinesterase and Butyrylcholinesterase inhibitors. *Comput. Biol. Chem.* **2018**, *74*, 304–326, https://doi.org/10.1016/j.compbiolchem.2018.03.021.
- Belkadi, A.; Kenouche, S.; Melkemi, N.; Daoud, I.; Djebaili, R. Molecular docking/dynamic simulations, MEP, ADME-TOX-based analysis of xanthone derivatives as CHK1 inhibitors. *Struct. Chem.* 2022, *33*, 833–858, https://doi.org/10.1007/s11224-022-01898-z.
- 47. Daoud, I.; Mesli, F.; Melkemi, N.; Ghalem, S.; Salah, T. Discovery of potential SARS-CoV 3CL protease inhibitors from approved antiviral drugs using: virtual screening, molecular docking, pharmacophore mapping evaluation and dynamics simulation. *J. Biomol. Struct. Dyn.* **2022**, *40*, 12574-12591, https://doi.org/10.1080/07391102.2021.1973563.
- 48. World Health Organization. Antimicrobial Resistance: Global Report on Surveillance; World Health Organization; **2014**.
- 49. Rakshit, T.; Haldar, A.; Jana, S.; Raha, S.; Saha, R.; Mandal, D. A brief review on the antimicrobial activity of transition metal complexes with N,O donor chelating ligand. *Results Chem.* **2023**, *6*, 101224, https://doi.org/10.1016/j.rechem.2023.101224.
- 50. Ajlouni, A.M.; Taha, Z.A.; Al Momani, W.; Hijazi, A.K.; Ebqa'ai, M. Synthesis, characterization, biological activities, and luminescent properties of lanthanide complexes with *N,N'*-bis(2-hydroxy-1-naphthylidene)-1,6-hexadiimine. *Inorg. Chim. Acta* **2012**, *388*, 120-126, https://doi.org/10.1016/j.ica.2012.03.029.
- 51. Abu-Dief, A.M.; Abdel-Rahman, L.H.; Abdelhamid, A.A.; Marzouk, A.A.; Shehata, M.R.; Bakheet, M.A.; Almaghrabi, O.A.; Nafady, A. Synthesis and characterization of new Cr(III), Fe(III) and Cu(II) complexes

- incorporating multi-substituted aryl imidazole ligand: Structural, DFT, DNA binding, and biological implications. *Spectrochim. Acta A: Mol. Biomol. Spectrosc.* **2020**, 228, 117700, https://doi.org/10.1016/j.saa.2019.117700.
- 52. Yassin, S.K.; Alshawi, J.; Salih, Z.A.M. Synthesis, characterization and cytotoxic activity study of Cu (II), Co (II), Mn (II), Ni (II) and Cr (III) Metal Complexes with new guanidine Schiff base against the hepatocellular Carcinoma (HCAM) cancer cell. *Egypt. J. Chem.* **2020**, *63*, 4005–4016, https://doi.org/10.21608/ejchem.2020.37893.2778.
- 53. Yakub, T.; Jain, B.; Asthana, A.; Singh, A.K.; Susan, A.B.H. Carbon-13 NMR. In Spectroscopy, 1st Edition; Jenny Stanford Publishing: New York, **2023**; pp. 93–122.
- 54. Refat, M.S.; Al-Azab, F.M.; Al-Maydama, H.M.A.; Amin, R.R.; Jamil, Y.M.S.; Kobeasy, M.I. Synthesis, spectroscopic and antimicrobial studies of La(III), Ce(III), Sm(III) and Y(III) Metformin HCl chelates. *Spectrochim. Acta A: Mol. Biomol. Spectrosc.* **2015**, *142*, 392–404, https://doi.org/10.1016/j.saa.2015.01.096.
- 55. Refat, M.S.; Al-Azab, F.M.; Al-Maydama, H.M.A.; Amin, R.R.; Jamil, Y.M.S. Synthesis and in vitro microbial evaluation of La(III), Ce(III), Sm(III) and Y(III) metal complexes of vitamin B6 drug. *Spectrochim. Acta A: Mol. Biomol. Spectrosc.* **2014**, *127*, 196–215, https://doi.org/10.1016/j.saa.2014.02.043.
- 56. Uddin, M.N.; Chowdhury, D.A.; Mase, N.; Rashid, M.F.; Uzzaman, M.; Ahsan, A.; Shah, N.M. Spectral and computational chemistry studies for the optimization of geometry of dioxomolybdenum(VI) complexes of some unsymmetrical Schiff bases as antimicrobial agent. *J. Coord. Chem.* **2018**, *71*, 3874–3892, https://doi.org/10.1080/00958972.2018.1533125.
- 57. Hossain, M.S.; Camellia, F.K.; Uddin, N.; Kudrat-E-Zahan, M.; Banu, L.A.; Haque, M.M. Synthesis, Characterization and Antimicrobial Activity of Metal Complexes of N-(4-methoxybenzylidene) Isonicotinohydrazone Schiff Base. *Asian J. Chem. Sci.* **2019**, *6*, 1–8, https://doi.org/10.9734/ajocs/2019/v6i118987.
- 58. Ganesan, M.; Arockiasamy, S. A review of titanium (IV) complexes of Schiff base ligands and their derivatives containing the donor atoms ONO, ONON, ONNO, and heterocyclic exhibiting biological activity covered over two decades along with the significance of molecular docking. *Discov. Chem.* **2025**, 2, 7, https://doi.org/10.1007/s44371-024-00064-0.
- 59. Satyendra, N.S.; Pratiksha, G.; Dimple, D.; Ripul, M.; Sheela, M.; Vijay, C. Catalytic Investigation of ε-caprolactone Polymerization through Schiff Base Titanium (IV) Complexes. *Curr. Indian Sci.* **2024**, 2, e2210299X302408, http://dx.doi.org/10.2174/012210299X302408240607073134.
- 60. Al-Selwi, N.A.; Al-Azab, A.M.; Jamil, Y.M.S.; Al-Azab, F.M.; Al-Ryami, A.M. Evaluation of the effectiveness of new mixed ligand complexes against the vector of Dengue fever Aedes aegypti (Diptera; Culicidae). *Eclet. Quím.* **2024**, *49*, e-1526, https://doi.org/10.26850/1678-4618.eq.v49.2024.e1526.
- 61. Sil, S.; Das, A.; Seal, I.; Mukherjee, S.; Roy, S. A toxicological evaluation for safety assessment of ruthenium-based diosmetin complex in rats. *Regul. Toxicol. Pharmacol.* **2023**, *137*, 105303, https://doi.org/10.1016/j.yrtph.2022.105303.
- 62. Roesky, H.W.; Andruh, M. The interplay of coordinative, hydrogen bonding, and π–π stacking interactions in sustaining supramolecular solid-state architectures.: A study case of bis(4-pyridyl)- and bis(4-pyridyl-Noxide) tectons. *Coord. Chem. Rev.* **2003**, *236*, 91–119, https://doi.org/10.1016/S0010-8545(02)00218-7.
- 63. Al-Hakimi, A.N.; Alotaibi, M.N.R.; Al-Gabri, N.A.; Alnawmasi, J.S. Biological evaluation of nano-sized novel Schiff base ligand-based transition metal complexes. *Results Chem.* **2023**, *6*, 101107, https://doi.org/10.1016/j.rechem.2023.101107.
- 64. Thakur, M.; Kumari, S.; Kumari, M. Integrated quantum chemical calculations, predictive toxicity assessment, absorption, distribution, metabolism, excretion and toxicity profiling and molecular docking analysis to unveil the therapeutic potential of non-oxovanadium(IV) and organotin(IV) complexes targeting breast cancer cells. *Int. J. Quantum Chem.* **2024**, *124*, e27438, https://doi.org/10.1002/qua.27438.
- 65. Sarkhel, S.; Desiraju, G.R. NH...O, OH...O, and CH...O hydrogen bonds in protein–ligand complexes: Strong and weak interactions in molecular recognition. *Proteins Struct. Funct. Bioinform.* **2004**, *54*, 247–259, https://doi.org/10.1002/prot.10567.
- 66. Chinnasamy, M.; Venkatesh, N.; Marimuthu, P.; Sathiyan, G.; Alharbi, S.A.; Venkatesan, G. Synthesis, characterization, and biological evaluation of novel bioactive Schiff base metal complexes and their molecular docking studies. *J. Environ. Chem. Eng.* **2025**, *13*, 115835, https://doi.org/10.1016/j.jece.2025.115835.

Publisher's Note & Disclaimer

The statements, opinions, and data presented in this publication are solely those of the individual author(s) and contributor(s) and do not necessarily reflect the views of the publisher and/or the editor(s). The publisher and/or the editor(s) disclaim any responsibility for the accuracy, completeness, or reliability of the content. Neither the publisher nor the editor(s) assume any legal liability for any errors, omissions, or consequences arising from the use of the information presented in this publication. Furthermore, the publisher and/or the editor(s) disclaim any liability for any injury, damage, or loss to persons or property that may result from the use of any ideas, methods, instructions, or products mentioned in the content. Readers are encouraged to independently verify any information before relying on it, and the publisher assumes no responsibility for any consequences arising from the use of materials contained in this publication.